Single-cell systems-level analysis of human Toll-like receptor activation defines a chemokine signature in patients with systemic lupus erythematosus

William E. O'Gorman, PhD,[a]*‖ Elena W. Y. Hsieh, MD,[a,b]* Erica S. Savig, BA,[c]‡ Pier Federico Gherardini, PhD,[a]‡ Joseph D. Hernandez, MD, PhD,[b,d] Leo Hansmann, PhD,[a] Imelda M. Balboni, MD, PhD,[b] Paul J. Utz, MD, PhD,[e,f] Sean C. Bendall, PhD,[d] Wendy J. Fantl, PhD,[a,g] David B. Lewis, MD,[b] Garry P. Nolan, PhD,[a,f]§ and Mark M. Davis, PhD[a,f,h]§ *Stanford, Calif*

Background: Activation of Toll-like receptors (TLRs) induces inflammatory responses involved in immunity to pathogens and autoimmune pathogenesis, such as in patients with systemic lupus erythematosus (SLE). Although TLRs are differentially expressed across the immune system, a comprehensive analysis of how multiple immune cell subsets respond in a system-wide manner has not been described.

Objective: We sought to characterize TLR activation across multiple immune cell subsets and subjects, with the goal of establishing a reference framework against which to compare pathologic processes.

Methods: Peripheral whole-blood samples were stimulated with TLR ligands and analyzed by means of mass cytometry simultaneously for surface marker expression, activation states of intracellular signaling proteins, and cytokine production. We developed a novel data visualization tool to provide an integrated view of TLR signaling networks with single-cell resolution. We studied 17 healthy volunteer donors and 8 patients with newly diagnosed and untreated SLE.

Results: Our data revealed the diversity of TLR-induced responses within cell types, with TLR ligand specificity. Subsets of natural killer cells and T cells selectively induced nuclear factor κ light chain enhancer of activated B cells in response to TLR2 ligands. CD14^{hi} monocytes exhibited the most polyfunctional cytokine expression patterns, with more than 80 distinct cytokine combinations. Monocytic TLR-induced cytokine patterns were shared among a group of healthy donors, with minimal intraindividual and interindividual variability. Furthermore,

From [a]the Department of Microbiology and Immunology, [b]the Department of Pediatrics, Division of Allergy, Immunology and Rheumatology, [c]the Cancer Biology Program, [d]the Department of Pathology, [e]the Department of Medicine, Division of Immunology and Rheumatology, [f]the Institute for Immunity, Transplantation and Infection, [g]the Department of Obstetrics and Gynecology, Division of Gynecologic Oncology, and [h]the Howard Hughes Medical Institute, Stanford University.

*These authors contributed equally to this work as co-first authors.

‡These authors contributed equally to this work as co-second authors.

§These authors contributed equally to this work as co-senior authors.

‖Dr O'Gorman is currently affiliated with ITGR/OMNI Biomarkers, Development Sciences, Genentech, South San Francisco, Calif.

E.W.Y.H. is a Fellow of the Pediatric Scientist Development Program; supported by the Eunice Kennedy Shriver National Institute of Child Health and Human Development grant K12 HD000850, the Lucile Packard Foundation for Children's Health Stanford CTSA UL1 TR001085, and the Child Health Research Institute of Stanford University. E.S.S. is a National Science Foundation Graduate Research Fellow and Gabilon Stanford Graduate Research Fellow. P.F.G. is a Howard Hughes Medical Institute Fellow of the Life Sciences Research Foundation. J.D.H. is funded by the American Academy of Allergy Asthma and Immunology Mylan Anaphylaxis Research Award. L.H. is funded by the German Research Foundation DFG, HA 6772/1-1. I.M.B. is supported by National Institutes of Health (NIH) grant K08 AI080945, the Stanford Child Health Research Institute, and the Arthritis Foundation Postdoctoral Fellowship. D.B.L. is supported by funds from NIH grants R01 AI083757 and R01 AI100121. S.C.B. is supported by the Damon Runyon Cancer Research Foundation Fellowship (DRG-2017-09) and NIH R00 GM104148-03. This work is supported by funds from NIH grants U19AI057229, U19AI090019, U54CA149145, T32AI007290, N01-HV-00242, 1R01CA130826, R01GM109836, 1R01NS089533, P01 CA034233, 1U19AI100627, 5R01AI073724, R01CA184968, R33CA183654, and R33CA183692; HHSN272201200028C, 201303028, HHSN272200700038C, 5U54CA143907, 1149112 NIH–Baylor Research Institute 41000411217; NIH–Northrop Grumman Corp 7500108142; the California Institute for Regenerative Medicine DR1-01477; the US Food and Drug Administration HHSF223201210194C; the Bill and Melinda Gates Foundation OPP1113682; the European Commission HEALTH.2010.1.2-1; the Alliance for Lupus Research 218518; an Entertainment Industry Foundation NWCRA grant; US Department of Defense grants OC110674 and 11491122; Rachford and Carlota A. Harris Endowed Professorship; and the Howard Hughes Medical Institute.

Disclosure of potential conflict of interest: W. E. O'Gorman has received research support from the National Institutes of Health (NIH; T32-AI007290) and has received personal fees as a paid speaker for DVS/Fluidigm Sciences. E. W. Y. Hsieh has received research support from the Pediatric Scientist Development Program (K12-HD000850) and the Lucile Packard Foundation for Children's Health (Stanford CTSA UL1 TR001085) and has received personal fees as a paid speaker for DVS/Fluidigm Sciences. E. S. Savig has received research support from the National Science Foundation Research Fellowship and the Gabilon Stanford Graduate Research Fellowship. P. F. Gherardini has received research support from the Life Sciences Research Foundation. J. D. Hernandez has received research support from the American Academy of Allergy, Asthma & Immunology. L. Hansmann has received research support from the German Research Foundation (DFG, HA 6772/1-1). I. M. Balboni has received research support from the NIH (K08-AI-080945), the Arthritis Foundation, and the Stanford Child Health Research Program Pilot Grant for Early Career Investigators. S. C. Bendall has received research support from the Damon Runyon Cancer Research Foundation (DRG-2017-09) and the NIH (R00 GM104148-03) and has received personal fees as a paid consultant for DVS Sciences. D. B. Lewis has received research support from the NIH (R01 AI083757 and R01 AI100121). G. P. Nolan has received research support from the NIH as follows: U19 AI057229, 1U19AI100627, U54 CA149145, N01-HV-00242, 1R01CA130826, 5R01AI073724, R01GM109836, R01CA184968, 1R01NS089533, P01 CA034233, R33 CA183654, R33 CA183692, 41000411217, 201303028, HHSN272201200028C, HHSN272200700038C, 5U54CA143907; CIRM DR1-01477; Department of Defense OC110674, 11491122; FDA HHSF223201210194C; Bill and Melinda Gates Foundation OPP1113682; Alliance for Lupus Research 218518; and a Rachford and Carlota A. Harris Endowed Professorship. Additionally, he has received support from DVS/Fluidigm Sciences and Becton Dickinson outside of the submitted work. M. M. Davis has received research support from the Howard Hughes Medical Institute and the NIH (U19-AI057229 and U19-AI090019). The rest of the authors declare that they have no relevant conflicts of interest.

Received for publication December 20, 2014; revised March 20, 2015; accepted for publication April 1, 2015.

Corresponding author: Garry P. Nolan, PhD, 269 Campus Drive, Center for Clinical Sciences Research 3205, Stanford, CA 94305-5175. E-mail: gnolan@stanford.edu. Or: Mark M. Davis, PhD, 279 Campus Dr, Beckman Center B221, Stanford, CA 94305-5175. E-mail: mmdavis@stanford.edu.

0091-6749

http://dx.doi.org/10.1016/j.jaci.2015.04.008

autoimmune disease altered baseline cytokine production; newly diagnosed untreated SLE patients shared a distinct monocytic chemokine signature, despite clinical heterogeneity.
Conclusion: Mass cytometry defined a systems-level reference framework for human TLR activation, which can be applied to study perturbations in patients with inflammatory diseases, such as SLE. (J Allergy Clin Immunol 2015;■■■:■■■-■■■.)

Key words: *Mass cytometry, Toll-like receptors, systemic lupus erythematosus, inflammation, monocytes, monocyte chemotactic protein 1*

Pattern recognition receptors (PRRs) recognize conserved features of foreign microorganisms during infection and self-molecules in tissue injury.[1,2] Toll-like receptors (TLRs) were the first identified family of PRRs; the human genome encodes 10 TLRs.[3,4] TLRs are type 1 transmembrane receptors with an extracellular ligand–binding domain, a transmembrane domain, and a cytoplasmic Toll/IL-1 receptor (TIR) domain.[3,5] TLRs are expressed on the plasma membrane (TLR1, TLR2, and TLR4-TLR6) or in endosomes (TLR3 and TLR7-TLR9).[6] Ligand binding to TLRs induces dimerization of the TIR domains. This dimer functions as a scaffold for myeloid differentiation primary response gene 88 (MyD88) or TIR domain–containing adaptor inducing IFN-β (TRIF) protein adaptor complexes, which then activate mitogen-activated protein kinase and nuclear factor κ light chain enhancer of activated B cells (NF-κB) pathways or interferon regulatory factors, respectively.[7,8] Crosstalk with other pathways elicits the production of inflammatory and regulatory cytokines that shape adaptive immunity.[9] Although TLR-induced inflammation is important for antimicrobial responses, inappropriate TLR recognition of self-molecules results in development of autoimmune diseases, such as systemic lupus erythematosus (SLE).[10,11] In patients with SLE, self-nucleic acid–containing antibodies form immune complexes that can sequentially activate Fcγ and endosomal TLR receptors.[12-14]

TLR signaling and cytokine production are precisely regulated at multiple levels to maintain the balance between protective immunity and inflammatory disease. First, the cellular compartmentalization of TLRs limits their accessibility to ligands. Second, different immune cell populations selectively express certain TLRs and TLR-inducible signaling pathways.[15] Finally, each immune cell subset produces a distinct set of cytokines. Systems-scale proteomic approaches have previously been applied to characterize this level of complexity of TLR networks. For example, mass spectrometry–based phosphoproteomic analysis was used to profile TLR-induced signaling in murine macrophages.[16,17] A separate study applied mass spectrometry–based secretomic analysis to evaluate cytokine production elicited by TLR activation in murine macrophages and dendritic cells.[18,19] Although informative, these studies have provided global views of TLR signaling and cytokine production in specific immune cell subsets but not within the context of an integrated cellular immune system with single-cell resolution.

To achieve a systems-level perspective of TLR biology that simultaneously accounts for functional diversity at the single-cell level, the activation of intracellular signaling pathways, and cytokine production, we capitalized on the ability of mass cytometry to capture this complexity. Here, 40-parameter mass cytometry was used to define a reference framework for human TLR activation *ex vivo* in whole blood samples. The application of this framework to evaluate cytokine alterations in a systemic inflammatory disease, such as SLE, revealed a characteristic abnormal monocytic chemokine signature in patients with SLE in the basal state in the absence of any *ex vivo* stimulation. This study demonstrates the utility of this approach to characterize TLR activation across the immune system and in patients with inflammatory diseases in general.

Abbreviations used
CD1c$^+$ DC: Conventional dendritic cell
CREB: cAMP response element–binding protein
MCP-1: Monocyte chemotactic protein 1
MIP-1β: Macrophage inflammatory protein 1β
MyD88: Myeloid differentiation primary response gene 88
NF-κB: Nuclear factor κ light chain enhancer of activated B cells
NK: Natural killer
PAM: Synthetic di (PAM2) or tri (PAM3) acylated lipoprotein
pDC: Plasmacytoid dendritic cell
PRR: Pattern recognition receptor
R848: Resiquimod
SLE: Systemic lupus erythematosus
TIR: Toll/IL-1 receptor
TLR: Toll-like receptor
TRIF: TIR domain–containing adaptor inducing IFN-β

METHODS

Study participants

All human donors were enrolled under a study protocol approved by the Institutional Review Board of the Research Compliance Office at Stanford University. Written informed consent was obtained from all study participants. Inclusion/exclusion criteria for healthy volunteer donors and patients with SLE can be found in the Methods section and Table E1 in this article's Online Repository at www.jacionline.org. Patients with SLE fulfilled the revised American College of Rheumatology diagnostic criteria (see Table E2 in this article's Online Repository at www.jacionline.org).[20]

Sample processing, stimulation, and cytometric analysis

Donor whole blood was collected in heparinized vacutainers (BD, Franklin Lakes, NJ), incubated at 37°C with TLR ligands[21] (see Table E3 in this article's Online Repository at www.jacionline.org), fixed, and permeabilized for intracellular staining. Conditions for signaling proteins and intracellular cytokine staining were adapted from previous studies (see the Methods section in this article's Online Repository).[22,23] Clone, vendor, and conjugation information for all mAbs are shown in Table E4 in this article's Online Repository at www.jacionline.org. Cells were analyzed on a CyTOF instrument (Fluidigm, South San Francisco, Calif). Data were acquired by using internal metal isotope bead standards, normalized, and analyzed as previously described (FlowJo software; TreeStar, Ashland, Ore and Cytobank, Mountain View, Calif).[24,25]

"Signaling network heatmap" visualization tool

In brief, for each experimental condition and cell type population, representative single cells were sampled and ordered from lowest to highest transformed value for each signaling protein. Subtractions between stimulated and unstimulated conditions yielded single-cell signaling fold changes, which were colored and packed together into a signaling node. See the

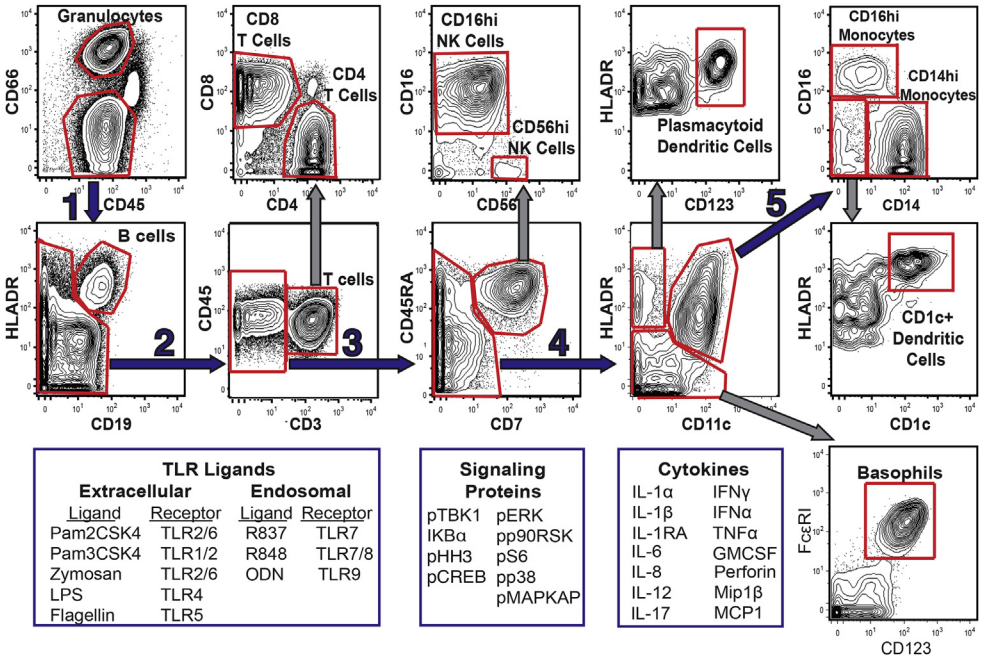

FIG 1. Mass cytometry identifies major immune cell subsets in human whole blood. After fixation and RBC lysis, cells were labeled with 22 surface markers that defined 11 general cell types. The extended T-cell gating strategy is shown in Fig E1. Subsequently, cells were permeabilized, stained with mAbs that probe intracellular proteins (see Table E4), and analyzed by means of mass cytometry. Representative data from 1 healthy donor are shown. *ODN*, Oligodeoxynucleotide; *pERK*, phosphorylated extracellular signal-regulated kinase; *pHH3*, phosphorylated histone H3; *pTBK1*, phosphorylated TANK-binding kinase 1.

Methods section in this article's Online Repository for data processing steps and visualization development.

CD14^{hi} monocytes combinatorial cytokine heatmap

In brief, cytokine positivity was determined in a binary fashion based on the 95th percentile intensity threshold; CD14^{hi} monocyte subpopulations expressing different cytokine combinations were clustered based on similar cytokine response profiles induced by TLR ligands. See the Methods section in this article's Online Repository for data processing and computational design.

Statistical analysis of CD14^{hi} monocyte cytokine signatures

Comparison of the mean percent positivity (defined by the 95th percentile threshold as above) for each monocytic cytokine between the SLE and healthy control groups was performed by applying a Student *t* test with Bonferroni adjustment, which apportions the significance level evenly among the 9 hypothesis tests ($P = .0056$, adjusted significance level; Microsoft Excel 2011).

RESULTS

Mass cytometry identifies major immune cell subsets in human whole blood

By using *a priori* knowledge about hematopoietic lineages, human blood cells were categorized into 11 major immune cell subsets (Fig 1 and see Fig E1 in this article's Online Repository at www.jacionline.org). Granulocytes, B cells, and T cells were classified based on surface marker expression of CD66, CD19/CD20/HLA-DR, and CD3, respectively.[22] CD3$^-$CD19$^-$HLA-DR$^-$CD7$^+$ lymphocytes[26] were subdivided into CD16^{hi} and CD56^{hi} natural killer (NK) cell subsets.[27] CD11c and HLA-DR coexpression defined nongranulocytic myeloid cells.[28] CD11c^{lo}HLA-DR^{hi}CD123$^+$ cells were classified as plasmacytoid dendritic cells (pDCs).[29] CD11c$^+$HLA-DR$^+$ monocytes were subdivided into CD14^{hi} (classical) and CD16^{hi} (nonclassical) subsets.[30] CD1c expression defined conventional dendritic cells (CD1c$^+$ DCs),[28] and FcεRI and CD123 coexpression identified basophils.[31] TLRs, their ligands, signaling pathways, and cytokines examined are listed in Fig 1.

A signaling network heatmap visualization tool provides an integrated view of TLR signaling patterns

Changes in the activation states of 9 signaling proteins were monitored in 11 cell subsets in response to 8 stimuli. Conventional depiction of such high-density data with 2-dimensional plots, histograms, or heatmaps does not capture an integrated view of all the measured parameters nor does it make the most of the single-cell resolution. A signaling network heatmap visualization tool was developed to overcome this analytic challenge. In brief, up to 1000 representative single cells were sampled from each immune cell subset and TLR stimulus condition. For each cell type and condition, cells were ordered by expression value for every signaling protein indexed from lowest to highest arcsinh transformed value. The arcsinh scale, a bioexponential transformation used with flow cytometric data, was chosen over a traditional log scale to account for negative values.[32] For each cell type and signaling protein, expression values for that signaling protein in the stimulated and unstimulated conditions were paired according to their indexed transformed value. Differences between these paired values

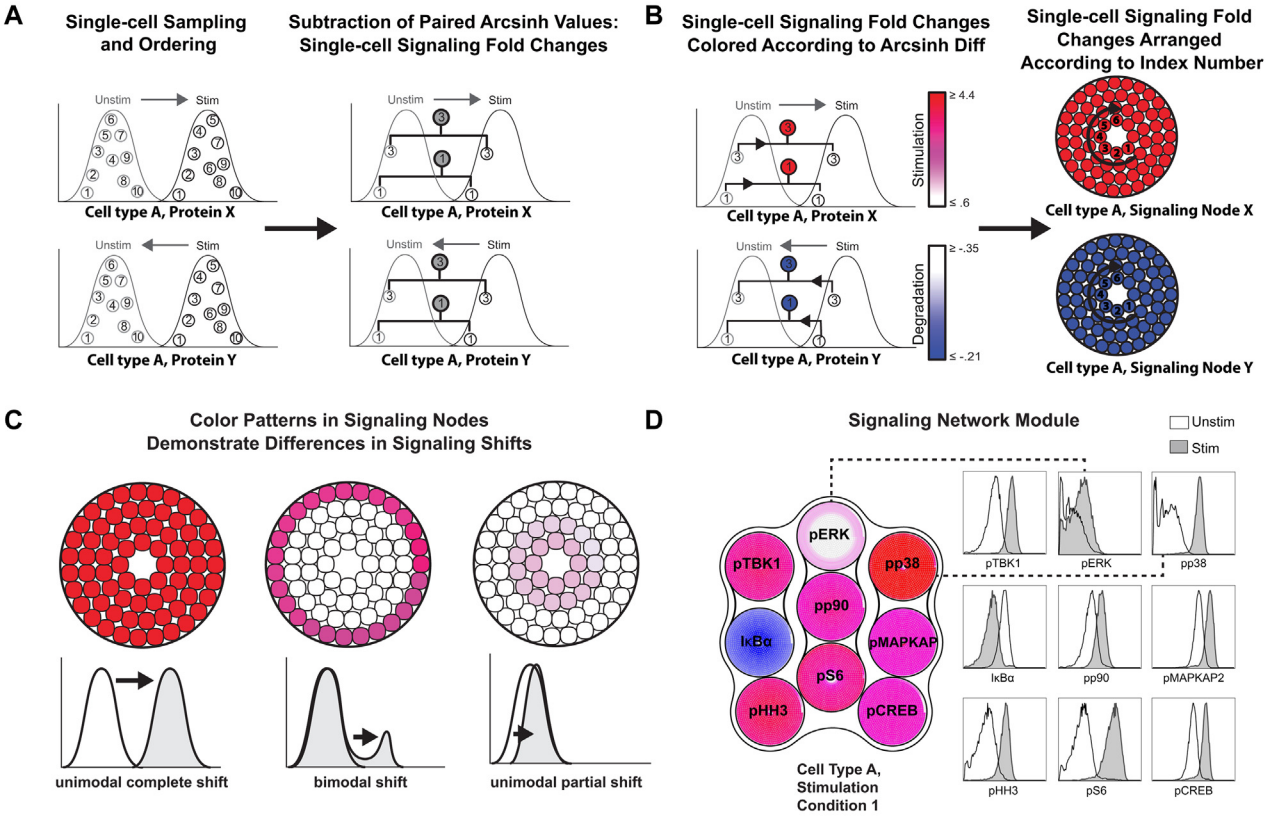
A
Single-cell Sampling and Ordering
Subtraction of Paired Arcsinh Values: Single-cell Signaling Fold Changes
Unstim
Stim
Cell type A, Protein X
Cell type A, Protein Y
B
Single-cell Signaling Fold Changes Colored According to Arcsinh Diff
Single-cell Signaling Fold Changes Arranged According to Index Number
Stimulation
≥ 4.4
≤ .6
Degradation
≥ -.35
≤ -.21
Cell type A, Signaling Node X
Cell type A, Signaling Node Y
C
Color Patterns in Signaling Nodes Demonstrate Differences in Signaling Shifts
unimodal complete shift
bimodal shift
unimodal partial shift
D
Signaling Network Module
Unstim
Stim
pERK
pTBK1
pp38
pp90
IκBα
pMAPKAP
pS6
pHH3
pCREB
pMAPKAP2
Cell Type A, Stimulation Condition 1

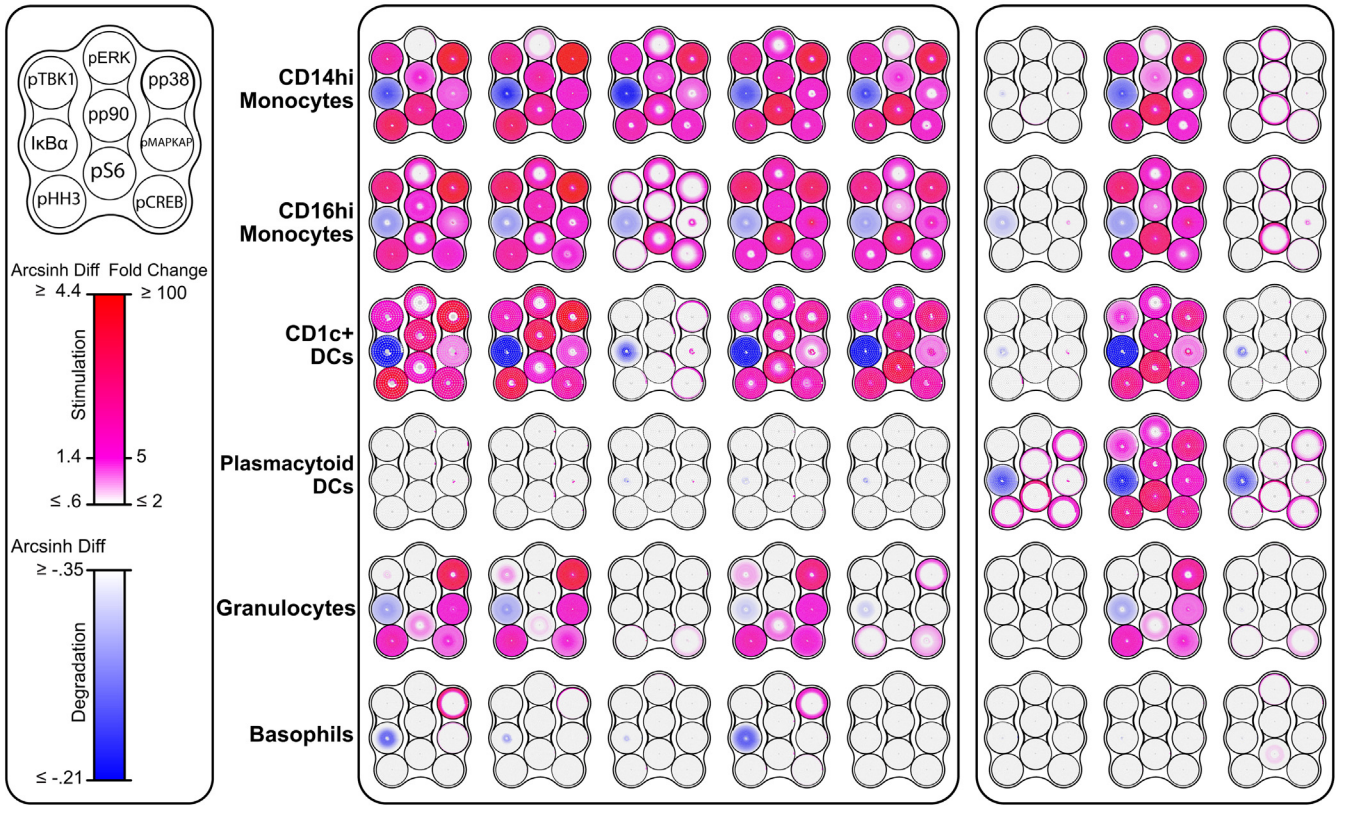
E
Extracellular TLR Ligands
Endosomal TLR Ligands
PAM2 TLR 2/6
PAM3 TLR 1/2
Zymosan TLR 2/6
LPS TLR 4
Flagellin TLR 5
R837 TLR 7
R848 TLR 7/8
ODN2006 TLR 9
CD14hi Monocytes
CD16hi Monocytes
CD1c+ DCs
Plasmacytoid DCs
Granulocytes
Basophils
Arcsinh Diff Fold Change
≥ 4.4
≥ 100
Stimulation
1.4
5
≤ .6
≤ 2
Arcsinh Diff
≥ -.35
Degradation
≤ -.21

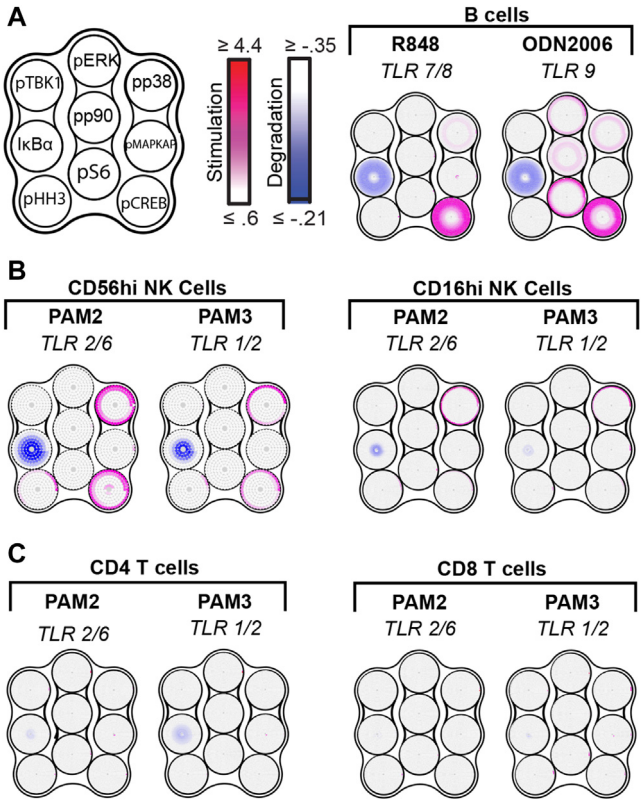

FIG 3. Signaling network heatmap demonstrates selective NF-κB activation in subsets of NK and T cells. **A,** B cells respond to endosomal stimuli with induction of the NF-κB pathway and CREB phosphorylation. **B** and **C**, Trace populations of NK cells (Fig 3, *B*) and T cells (Fig 3, *C*) responded to PAM2 and PAM3, with induction of the NF-κB pathway. Representative data from 1 healthy donor are shown. For the complete lymphoid single-cell heatmap, see Fig E4. For additional experiments involving purified NK and T-cell populations and their TLR2 responses from additional donors, see Figs E5-E7. *ODN*, Oligodeoxynucleotide; *pERK*, phosphorylated extracellular signal-regulated kinase; *pHH3*, phosphorylated histone H3; *pS6*, phosphorylated ribosomal S6 kinase; *pTBK1*, phosphorylated TANK-binding kinase 1.

resulted in single-cell signaling fold changes (Fig 2, *A*), which were colored according to the arcsinh difference (Fig 2, *B*) and arranged into a signaling node (Fig 2, *C*) based on their original index position. These signaling nodes were then arranged into pathways downstream of MyD88 and TRIF adaptor protein complexes (Fig 2, *D*). The generalized pathways include NF-κB and activator protein 1 activation, as well as proteins involved in downstream transcriptional and translational regulation (for further details, see the Methods section in this article's Online Repository). Signaling network heatmap and variance data from other donors are shown in Figs E2 and E3 in this article's Online Repository at www.jacionline.org, respectively.

Systems-level TLR signaling analysis demonstrates diverse signaling responses in myeloid cell subsets and selective NF-κB activation in NK and T-cell subsets

In the myeloid lineage the induction of every measured signaling protein was observed in more than 95% of $CD14^{hi}$ and $CD16^{hi}$ monocytes in response to all extracellular TLR ligands and the endosomal TLR7/8 ligand resiquimod (R848; 15- to 100-fold increases with marginal activation of phosphorylated extracellular signal-regulated kinase; Fig 2, *E*). Although pDCs only responded to endosomal stimuli, $CD1c^{+}$ DC TLR signaling responses largely overlapped with monocytic signaling responses, with the exception of zymosan. Zymosan induced IκBα degradation in both $CD1c^{+}$ DCs and $CD14^{hi}$ monocytes. However, zymosan also activated multiple other signaling pathways in $CD14^{hi}$ monocytes. This difference is potentially due to the fact that $CD1c^{+}$ DCs express TLR2 only, whereas $CD14^{hi}$ monocytes express both TLR2 and dectin-1 receptors.[33] Like $CD1c^{+}$ DCs, granulocytes responded to all extracellular ligands and R848 (Fig 2, *E*). In contrast, only a fraction of basophils responded to PAM2 (TLR2/6 ligand; 15.5% responders) and LPS (TLR4 ligand; 7.2% responders) with induction of IκBα degradation and p38 phosphorylation (Fig 2, *E*). This restricted basophil-signaling profile is concordant with previous studies on the roles of TLR2- and TLR4-mediated basophil activation in augmenting allergic reactions.[34]

In the lymphoid lineage endosomal TLR agonists induced NF-κB and cAMP response element–binding protein (CREB) pathways in B cells (Fig 3, *A*, and see Fig E4 in this article's Online Repository at www.jacionline.org). Unexpectedly, the TLR2 ligands PAM2 (TLR2/6) and PAM3 (TLR1/2) selectively activated the NF-κB pathway in NK and T-cell subsets (Fig 3, *B* and *C*). In approximately one third of $CD56^{hi}$ NK cells, IκBα

FIG 2. A signaling network heatmap visualization tool provides an integrated view of TLR signaling patterns. **A,** Up to 1000 representative cells were sampled for each cell type population and for unstimulated *(unstim)* and stimulated *(stim)* conditions. Cells were ordered from the lowest to highest arcsinh transformed value for each signaling protein. Corresponding single-cell arcsinh values between unstimulated and stimulated cells were subtracted on a pairwise basis, which constitute single-cell signaling fold changes. **B,** These single-cell signaling fold changes are indexed in the same numbered order as the cells from which they were derived and colored in red (phosphorylation) or blue (protein degradation), according to their arcsinh difference value. Single-cell signaling fold changes are arranged according to their index number from lowest to highest, starting from the inside and moving clockwise to form a signaling node. **C,** Signaling nodes demonstrate the distribution of responsive cells in a given population. The center of the node corresponds to the lowest values of the histograms, and the periphery corresponds to the highest values. Model activation patterns are shown. **D,** Signaling nodes are organized in a signaling network module, reflecting a generalized structure of TLR response pathways. **E,** Human whole blood was stimulated with the TLR ligands indicated in Fig 1. After stimulation, cells were fixed, stained, analyzed, and classified as described in Fig 1. Single-cell signaling fold changes were derived and organized as described above. Signaling data from 1 healthy donor are shown; additional donors and variances from other sampled donors are shown in Figs E2 and E3. *ODN*, Oligodeoxynucleotide; *pERK*, phosphorylated extracellular signal-regulated kinase; *pHH3*, phosphorylated histone H3; *pS6*, phosphorylated ribosomal S6 kinase; *pTBK1*, phosphorylated TANK-binding kinase 1.

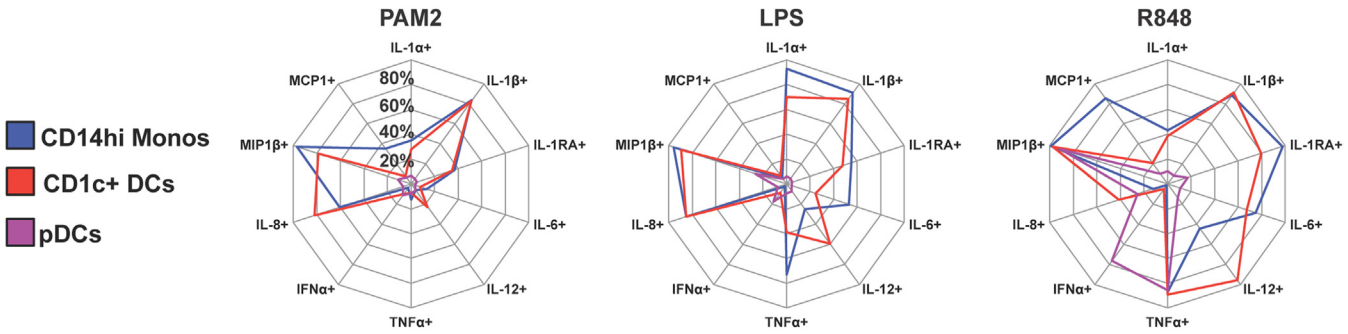

FIG 4. TLR-induced cytokine signatures demonstrate TLR agonist and cell type specificity. Human whole blood was stimulated with PAM2, LPS, and R848 for 6 hours in the presence of protein secretion inhibitors. Monocytes *(Monos)* and dendritic cells were identified, as indicated in Fig 1. Cells demonstrating cytokine production levels greater than the 95th percentile of unstimulated cells were defined as cytokine positive (see Fig E8). Cytokine signatures are presented as radar plots with 20% radial intervals. Cytokines are arranged in functional families in clockwise order: IL-1 family (IL-1α, IL-1β, and IL-1 receptor antagonist), proinflammatory cytokines (IL-6, IL-12, TNF-α, and IFN-α), and chemokines (MIP-1β, MCP-1, and IL-8). Average values based on responses from 9 healthy donors are shown. Cytokine variance data are shown in Fig E11.

degradation (36.6% responders) was observed in response to PAM2 stimulation (also phosphorylation of pCREB and p38; see Fig E5, *A*, in this article's Online Repository at www.jacionline.org). A lower frequency of $CD56^{hi}$ NK cells (20.1%) responded to PAM3 stimulation (see Fig E5, *A*). These responses were far less apparent in $CD16^{hi}$ NK cells (Fig 3, *B*, and see Fig E5, *B*). PAM2 and PAM3 stimulations were performed in 10 additional donor blood samples, resulting in IκBα degradation in 36% (SD, 12.67%) and 24.3% (SD, 17%) of $CD56^{hi}$ NK cells, respectively (see Fig E5, *B*), to assess the reproducibility of this observation. NK cells were enriched to approximately 96.75% purity (see the Methods section in this article's Online Repository) and stimulated with PAM2 and PAM3 to understand this further. IκBα degradation was mainly observed in the $CD56^{hi}$ NK population in response to PAM2, suggesting that this TLR ligand directly activated these cells (see Fig E6 in this article's Online Repository at www.jacionline.org).

As observed for NK cells, PAM2 and PAM3 stimulation also activated the NF-κB pathway in CD4 T cells (Fig 3, *C*). This activity was even less apparent in CD8 T cells (Fig 3, *C*, and see Fig E7, *A*, in this article's Online Repository at www.jacionline.org). In a group of 10 additional donors, an average of 14.5% (SD, 5.1%) and 11.9% (SD, 7.8%) CD4 T cells responded to PAM2 and PAM3, respectively (see Fig E7, *B*). To investigate whether PAM2 and PAM3 directly activated T cells, T cells enriched to approximately 96% purity were stimulated with these ligands, and exclusive NF-κB pathway induction was observed in similar percentages of cells (average of 14.03% and SD of 5.1% for PAM2 and average of 4.32% and SD of 5.1% for PAM3; see Fig E7, *C*), indicating that these lipopeptides are acting directly on T lymphocytes. Although previous studies have explored the role of TLR2 agonists in T-cell activation,[35,36] activation of specific signaling pathways has not been well defined.

TLR-induced cytokine signatures demonstrate cell type and TLR ligand specificity

Production of 16 cytokines downstream of the signaling pathways examined above was simultaneously measured in myeloid and lymphoid cell types (Fig 1). Cytokine data were analyzed by using a Boolean gating strategy, with positivity defined in Fig E8 in this article's Online Repository at www.jacionline.org. TLR stimulation induced the production of 10 of 16 cytokines in 1 or more myeloid cell populations, with minimal cytokine production in lymphoid cells (Fig 4 and see Fig E9 in this article's Online Repository at www.jacionline.org).

Mirroring TLR-induced signaling patterns, $CD14^{hi}$ monocyte and $CD1c^{+}$ DC cytokine response profiles also largely overlapped (Fig 4 and see Fig E10 in this article's Online Repository at www.jacionline.org). However, $CD1c^{+}$ DCs consistently produced more IL-12 (35.7% more, averaged over all TLR ligand conditions) after stimulation than did $CD14^{hi}$ monocytes (see Fig E10). LPS and R848 induced different chemokine responses in $CD14^{hi}$ monocytes, and LPS elicited IL-8 production in the absence of monocyte chemotactic protein 1 (MCP-1) expression, whereas R848 induced the converse (Fig 4). $CD16^{hi}$ monocytes were not included in the cytokine analysis because after the 6-hour stimulation period, CD16 was shed from nonclassical monocytes.

Unlike monocytes and $CD1c^{+}$ DCs, pDCs demonstrated a restricted cytokine response repertoire, primarily IFN-α production in response to endosomal TLR agonists (Fig 4). Granulocytes and basophils produced macrophage inflammatory protein 1β (MIP-1β), IL-8, and IL-1 receptor antagonist only (see Fig E9, *A*). Minimal cytokine production was observed in the lymphoid compartment (see Fig E9, *B*), even for B cells, in which endosomal TLR stimulation induced signaling responses (Fig 3, *A*). Despite the PAM2- and PAM3-driven NF-κB signaling activation observed in NK and T-cell subpopulations (Fig 3, *B* and *C*), cytokine responses were not induced in these cells (see Fig E9, *B*), suggesting that these TLR ligands play a costimulatory role in antigen receptor activation.

TLR ligands induce diverse combinatorial cytokine signatures in $CD14^{hi}$ monocytes

Combinatorial cytokine production is the ability to produce numerous combinations of cytokines simultaneously. T cells have been shown to exhibit combinatorial polyfunctional cytokine responses that are correlated with resistance to disease.[37,38]

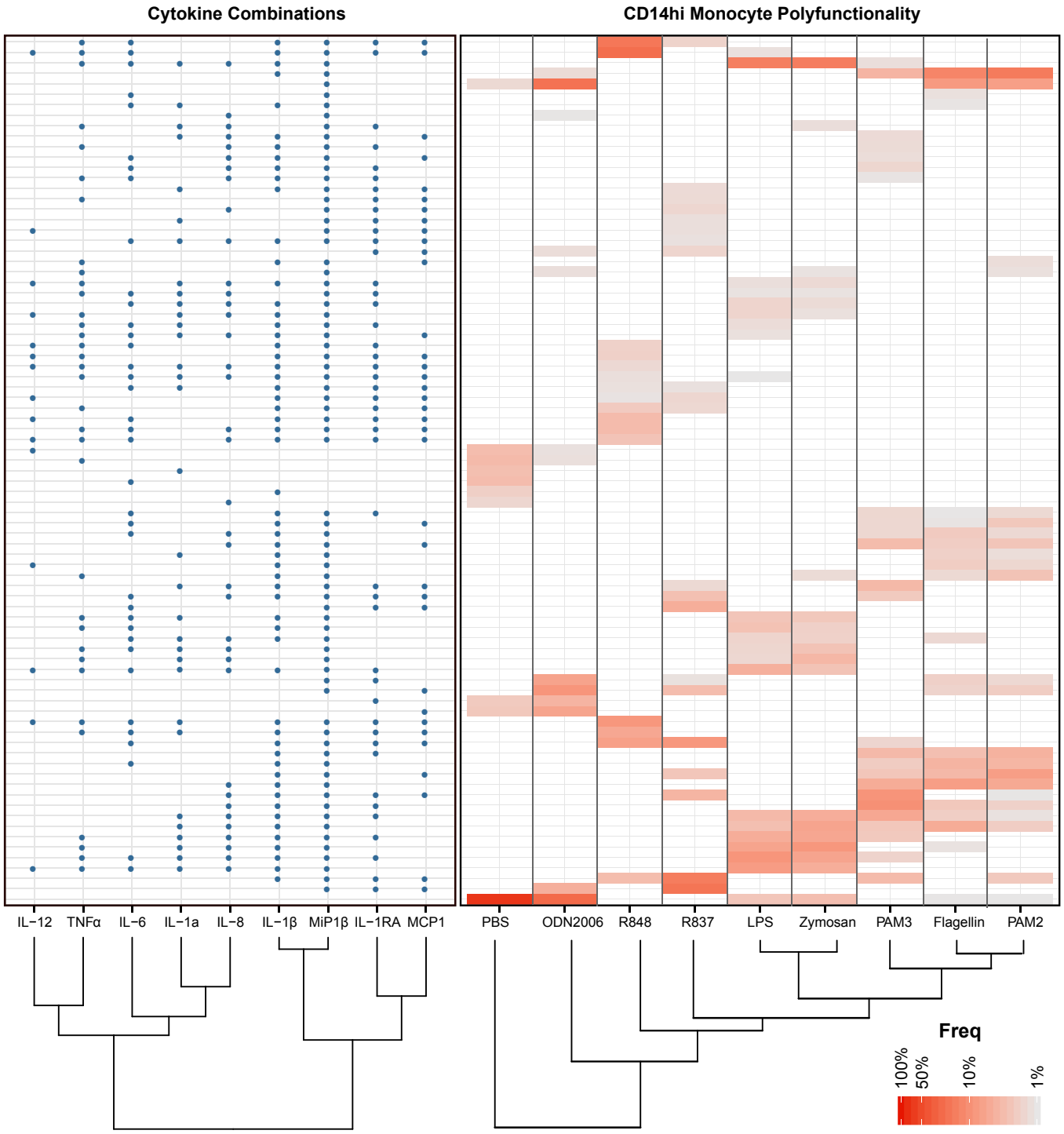

FIG 5. TLR ligands induce diverse combinatorial cytokine signatures in $CD14^{hi}$ monocytes. $CD14^{hi}$ monocyte combinatorial cytokine polyfunctionality was assessed in response to 8 TLR ligands listed in Fig 1. A Boolean gating script was used to quantify subgroup frequency based on a 95th percentile threshold (see Fig E8). Cytokine combinations are represented as *rows on the left panel*, with *blue dots* indicating positivity for a particular cytokine. For a 9-cytokine analysis, 512 possible combinations of coexpressed cytokines are possible. Only cytokine combinations expressed by more than 1% of cells are depicted; 83 different cytokine combinations were detected at this level and above. *Red color* scaling indicates the frequency of each $CD14^{hi}$ monocyte subpopulation. Hierarchic clustering of cytokines and TLR ligands relate cytokine coexpression patterns *(left panel)* and cytokine combination patterns shared between TLR ligands *(right panel)*, respectively. Data from 1 healthy donor are shown.

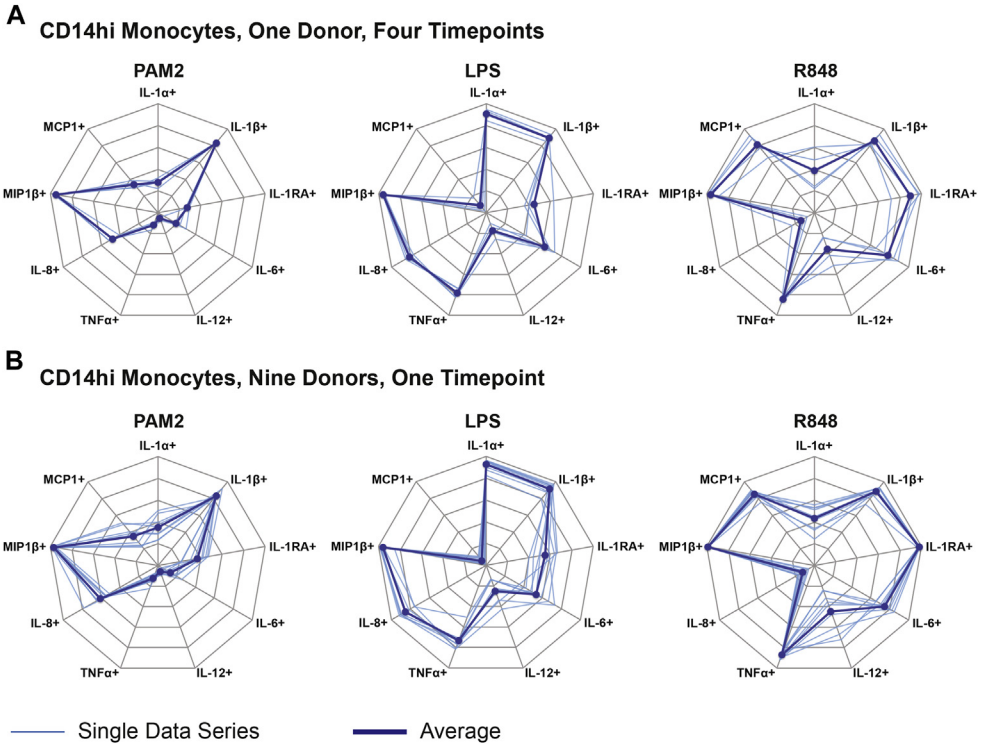

FIG 6. Intraindividual and interindividual reproducibility of TLR-induced cytokine signatures in healthy donor CD14^{hi} monocytes. **A,** *Thin lines* relate longitudinal monthly blood draw samples for 1 healthy donor. *Bold lines* relate the average of all 4 samples. **B,** *Thin lines* are specific to each distinct healthy donor. *Bold lines* represent the average of all 9 healthy donor cytokine responses.

However, it is not clear whether myeloid cell populations share this capability. In this study CD14^{hi} monocytes produced the most diverse cytokine responses to TLR stimulation (Fig 4 and see Fig E10). Only subsets with a minimum 1% population frequency were included in the analysis to emphasize salient polyfunctional combinations. Here we found that 83 of the possible 512 combinations meet that threshold (Fig 5). Hierarchic clustering of these cytokines into a combinatorial heatmap exposed relationships between coexpressed cytokines (Fig 5, left panel) and between TLR stimuli that elicit similar cytokine responses (Fig 5, right panel). IL-1β and MIP-1β behaved the most similarly, and the proinflammatory cytokines IL-12 and TNF-α formed a separate cluster.

PAM2, PAM3, and flagellin elicited similar cytokine profiles; generally, 2 or 3 cytokines were expressed, primarily IL-1β, MIP-1β, and IL-8 (Fig 5, right panel). LPS and zymosan also induced similar combinatorial cytokine signatures, likely related to the synergistic effects of dectin-1 with TLR2 and TLR4.[33] R848 and LPS induced comparable monocytic polyfunctionality (Fig 5, right panel) but differed in the type of cytokines induced (Fig 5, left panel). These cytokine combinatorial phenotypes suggest a monocytic functional specialization that cannot be defined by surface marker–based classifications alone.

CD14^{hi} monocytes from patients with SLE show an inflammatory cytokine signature typified by MCP-1

Intraindividual and interindividual variabilities in healthy donors were determined to assess the reproducibility of this approach for evaluating TLR-induced cytokine production. Monocytic TLR-induced cytokine patterns were highly conserved over time for a single donor (Fig 6, *A*) and among 9 healthy donors (Fig 6, *B*). The least degree of intraindividual and interindividual variability was observed for MIP-1β production, with the SD ranging from 1.02% (LPS) to 5.25% (R848) for 1 donor over time and 0.41% (R848) to 4.44% (LPS) among 9 donors (see Fig E11 in this article's Online Repository at www.jacionline.org). IL-12 production varied most, with an SD of 13.3% for 1 donor longitudinally and 18.2% for 9 donors in the R848 condition (see Fig E11). These results demonstrate the reproducibility of this experimental platform and validate the data as a reference framework of TLR-induced cytokine profiles in healthy donors. This reference framework was used to compare cytokine profiles in patients with an inflammatory disease in which abnormal TLR responses drive pathologic cytokine production, such as SLE.[39,40]

Analysis of blood samples from 8 patients with newly diagnosed, untreated, and clinically heterogeneous SLE (see Table E2) revealed a common abnormal CD14^{hi} monocytic cytokine signature in the basal state in the absence of *ex vivo* stimulation (Fig 7). Ninety-fifth percentile baseline thresholds (see Fig E7) for all cytokines were defined based on an initial time point when blood was immediately processed after draw (time zero, see Fig E10) to internally control these experiments. CD14^{hi} monocytes from each of the 8 patients with newly diagnosed and untreated SLE exhibited increased MCP-1 levels (average, 82.6%; SD, 9.7%; see Fig E8) after 6 hours of secretion block in the absence of any stimulation. Under these conditions, MCP-1 levels in corresponding healthy control subjects (different healthy donors than those in Fig 6) did not change to the same extent (average, 18.8%; SD, 8.1%; see Fig E12 in this article's Online Repository at www.jacionline.org). MCP-1 is an inducible

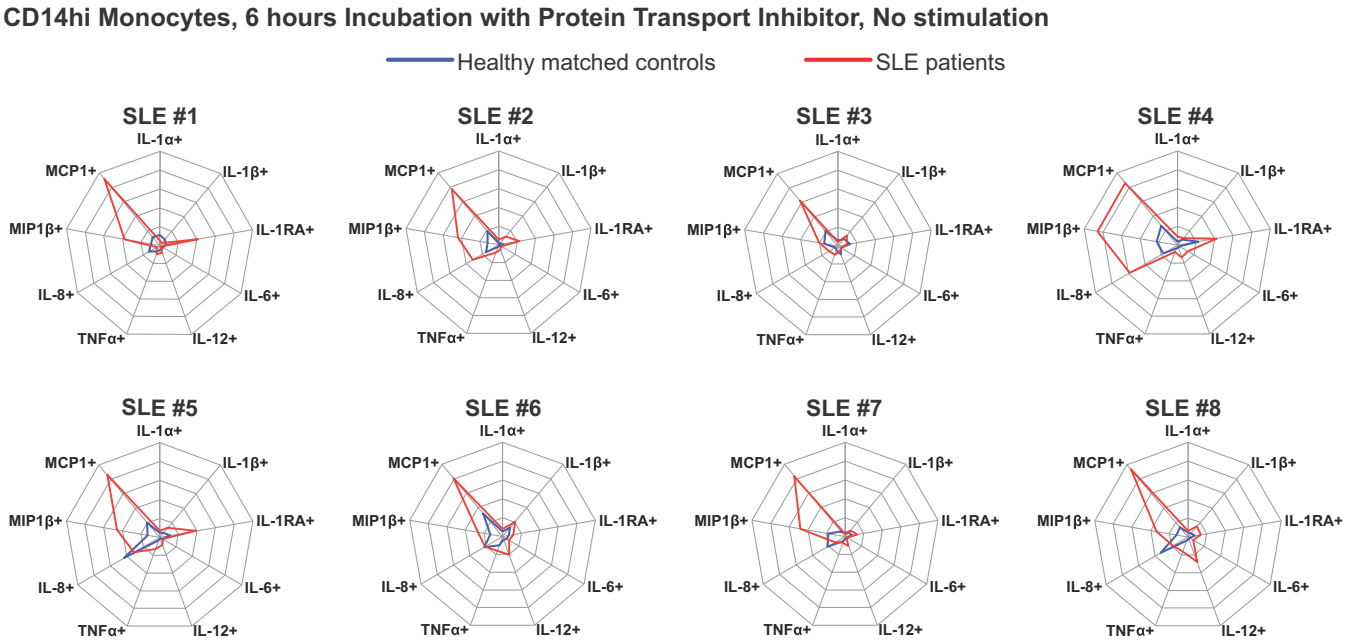

FIG 7. CD14^{hi} monocytes from patients with SLE show an inflammatory chemokine signature typified by MCP-1. Cytokine positivity was defined based on the 95th percentile threshold of blood processed immediately after draw (time zero) and thus were internally controlled. Each radar plot represents the CD14^{hi} monocytic cytokine signature of a patient with SLE *(red line)* versus a healthy sex-matched control subject *(blue line)* after a 6-hour incubation period with protein secretion inhibitor (no exogenous stimuli).

proinflammatory chemokine involved in the immunopathogenesis of human and murine lupus nephritis.[41] In murine SLE models MCP-1 inhibition ameliorates lupus nephritis.[42] Previous studies and our data indicate that MCP-1 holds promise as a therapeutic target.[42-45]

Levels of other cytokines, such as MIP-1β and TNF-α, were also increased in samples from patients with newly diagnosed and untreated SLE compared with those in healthy donor samples (Fig 7 and see Fig E13 in this article's Online Repository at www.jacionline.org). Bonferroni-adjusted *t* test calculation comparing the average expression of each cytokine between the SLE and healthy control groups confirmed statistically significant differences in MCP-1 ($P = 7.6E^{-10}$), MIP-1β ($P = .002$), and TNF-α ($P = .001$) levels. Comparison of cytokine profiles for all 11 cell subsets (as in Fig 1) for all 8 SLE versus healthy matched control pairs did not demonstrate any statistically significant differences other than those observed in CD14^{hi} monocytes (data not shown). Although all samples from patients with SLE demonstrated this common monocytic cytokine signature (MCP-1, MIP-1β, and TNF-α) based on single cytokine positivity (Fig 7), patients' combinatorial cytokine profiles differed (see Fig E14 in this article's Online Repository at www.jacionline.org).

In this study, using a systems-scale single-cell proteomic approach to characterize human TLR signaling and cytokine networks, we defined a reference framework that can be applied to study alterations in these parameters in patients with inflammatory disease.

DISCUSSION

TLRs (and other PRRs) are involved in the complex balance between protective immunity and inflammatory disease. To elucidate how TLR networks calibrate innate and adaptive immune responses to maintain this balance, we have used high-dimensional mass cytometry to broadly measure intracellular signaling responses and cytokine profiles in healthy subjects and patients with newly diagnosed and untreated SLE.

This comprehensive TLR activation analysis in healthy subjects corroborates previous findings in TLR biology and reveals novel TLR signaling responses in NK and T cells. A signaling network heatmap visualization tool (Fig 2, *A-D*) was developed to depict these TLR-induced signaling patterns with single-cell resolution. This method enables display of the activation characteristics of 9 signaling proteins in 11 cell subsets in response to 8 TLR ligands, with more than 600 features and approximately 2 million data points in Fig 2, *E*. This is a scalable tool to visualize high-dimensional data sets that provides a framework through which the signaling biology of entire receptor systems can be explored with nearly single-cell resolution.

Although TLR responses have been extensively investigated in myeloid cells, they are not well defined in the lymphoid lineage, with the exception of B cells.[46] In our analysis only TLR2 and TLR5 ligands activated signaling, primarily in CD56^{hi} NK cells (Fig 3, *B*). TLR2-dependent NK cell activation has been linked to poxvirus and mycobacterial immunity.[47,48] Notably, TLR2-mediated mycobacterial recognition promotes NK cell–DC cross-talk and IL-12 production,[49] but it is unclear whether TLR2 stimuli directly activated NK cells. It is unlikely that the observed signaling responses (Figs 2, *E*, and 3) were indirect (paracrine) in nature, given a 30-minute incubation; however, indirect effects cannot be completely excluded. Therefore purified cell populations were assayed to evaluate noncanonical TLR ligand responses in NK cells and T cells. Here we found that an enriched NK cell population responded to TLR2 ligands within 30 minutes, showing that NK cells can directly respond to these ligands (see Fig E6).

Similarly, TLR responses in T cells are also poorly described. A subset of CD4 T cells degraded IκBα after TLR2 stimulation (Fig 3, *C*), but this did not lead to cytokine production (see Fig E9, *B*). This pathway selectivity and the inability of TLR2 ligands alone to induce cytokine production in T cells suggest a costimulatory role for TLR2 in T-cell activation. This observation is consistent with and might provide a molecular mechanism for previous reports that mycobacterial ligands and the live BCG vaccine enhance T-cell proliferation and cytokine production only when coupled with T-cell receptor engagement.[36,50] These results also suggest that microbial lipopeptides should be explored as adjuvants in vaccine design. Detailed NK cell and T-cell phenotyping could be incorporated in future studies to further understand this isolated signaling response to TLR2 ligands.

TLR activation was tracked from signal transduction to cytokine production, demonstrating how different TLR agonists elicited distinct cytokine combinations across the immune system. To construct a systems-level TLR activation reference framework, we compared TLR-induced cytokine responses longitudinally in a single donor and among healthy donors. Minimal intraindividual and interindividual variability (Fig 6) suggested the applicability of this framework to study an inflammatory disease, such as SLE. Compared with monocytes from healthy control subjects, $CD14^{hi}$ monocytes from 8 patients with newly diagnosed and untreated SLE exhibited a statistically significant distinct cytokine signature (MCP-1, MIP-1β, and TNF-α) at the basal state, with the most prominent and uniform of the cytokines being MCP-1 (Fig 7 and see Fig E13). These 8 patients with SLE manifested diverse clinical symptoms (see Table E2), which is characteristic of this complex autoimmune disorder. Yet, significantly, by using our analysis system, they all expressed this cytokine signature, particularly MCP-1, suggesting that they shared an underlying basis that could be useful in both diagnosis and treatment. Additionally, these patient samples were obtained before any immunomodulatory treatment, and thus there was no heterogeneity introduced by drug treatments.

MCP-1 (also known as CCL2) recruits monocytes and lymphocytes to sites of inflammation.[45] Increased MCP-1 levels have been detected in patients with a variety of autoimmune disorders[51-53] and often correlate with disease activity.[43,45,54] MCP-1 might play a critical role in autoimmune end-organ damage, and MCP-1 neutralization has been shown to ameliorate disease in rodent models of SLE.[42] The mechanism responsible for increased MCP-1 production in patients with SLE is unclear, but available data suggest several possibilities.

First, MCP-1 is a known type I interferon inducible chemokine.[55] Multiple transcriptomic studies have observed an IFN-α signature in patients with SLE, likely induced by nucleic acid–containing immune complexes activating endosomal TLRs in pDCs[12,56] and possibly leading to MCP-1 induction. Second, Fcγ receptor activation elicits monocytic MCP-1 production,[57] and thus circulating immune complexes in patients with SLE could explain MCP-1 induction.[14] Finally, although RNA-containing immune complexes in patients with SLE might activate TLR8 in monocytes, leading to MCP-1 production, monocytic cytokine profiles from patients with SLE did not match R848-induced cytokine profiles, making this explanation unlikely. Regardless of the cause of MCP-1 production, MCP-1 neutralization could potentially serve as an anti-inflammatory adjunctive therapy to reduce the use or dosage of cytotoxic immunosuppressive drug regimens that are necessary to control SLE.

In conclusion, mass cytometry was used to generate a comprehensive reference framework of human TLR-driven immune responses in myeloid and lymphoid lineages. Analysis of samples from patients with SLE demonstrated that this reference framework could be applied to study inflammatory disease. Additionally, this study establishes a paradigm for using high-dimensional single-cell proteomic approaches to generate reference maps of other receptor systems.

We thank Zachary B. Bjornson, Monica Nicolau, Nima Aghaeepour, Tiffany J. Chen, and Karen Sachs for their assistance in data analysis. We thank John S. Tamaresis and Karen Sachs for their assistance with statistical analysis and Cristina Tato for helpful discussions. We thank Michael D. Leipold from the Human Immune Monitoring Core (HIMC), Angelica Trejo, and Astraea Jager for their intellectual and technical contributions.

Key messages

- **Mass cytometry demonstrates conserved cell type– and receptor-specific TLR activation signatures in healthy donors.**
- **Application of this systems-scale approach to interrogate inflammatory disease reveals an altered monocytic chemokine signature in newly diagnosed patients with SLE.**

REFERENCES

1. Ishii KJ, Koyama S, Nakagawa A, Coban C, Akira S. Host innate immune receptors and beyond: making sense of microbial infections. Cell Host Microbe 2008;3:352-63.
2. Akira S, Umeatsu S, Takeuchi O. Pathogen recognition and innate immunity. Cell 2006;124:783-801.
3. Netea MG, Wijmenga C, O'Neill LAJ. Genetic variation in Toll-like receptors and disease susceptibility. Nat Immunol 2012;13:535-42.
4. O'Neill LAJ, Golenbock D, Bowie AG. The history of Toll-like receptors —redefining innate immunity. Nat Rev Immunol 2013;13:453-60.
5. Beutler B, Eidenschenk C, Crozat K, Imler J-L, Takeuchi O, Hoffmann JA, et al. Genetic analysis of resistance to viral infection. Nat Rev Immunol 2007;7:753-66.
6. Blasius AL, Beutler B. Intracellular Toll-like receptors. Immunity 2010;32:305-15.
7. Takeuchi O, Akira S. Pattern recognition receptors and inflammation. Cell 2011;140:805-20.
8. Fitzgerald KA, Chen ZJ. Sorting out Toll signals. Cell 2006;125:834-6.
9. Iwasaki A, Medzhitov R. Regulation of adaptive immunity by the innate immune system. Science 2010;327:291-5.
10. Theofilopoulos AN, Gonzalez-Quintial R, Lawson BR, Koh YT, Stern ME, Kono DH, et al. Sensors of the innate immune system: their link to rheumatic diseases. Nat Rev Rheumatol 2010;6:146-56.
11. Kawasaki T, Kawai T, Akira S. Recognition of nucleic acids by pattern-recognition receptors and its relevance in autoimmunity. Immunol Rev 2011;243:61-73.
12. Ronnblom L, Pascual V. The innate immune system in SLE: type I interferons and dendritic cells. Lupus 2008;17:394-9.
13. Pascual V, Farkas L, Banchereau J. Systemic lupus erythematosus: all roads lead to type I interferons. Curr Opin Immunol 2006;18:676-82.
14. Means TK, Latz E, Hayashi F, Murali MR, Golenbock DT, Luster AD. Human lupus autoantibody–DNA complexes activate DCs through cooperation of CD32 and TLR9. J Clin Invest 2005;115:407-17.
15. Kawai T, Akira S. The role of pattern-recognition receptors in innate immunity: update on Toll-like receptors. Nat Immunol 2010;11:373-84.
16. Weintz G, Olsen JV, hauf KFU, Niedzielska M, Amit I, Jantsch J, et al. The phosphoproteome of Toll-like receptor-activated macrophages. Mol Syst Biol 2010;6:1-16.

17. Sjoelund V, Smelkinson M, Nita-Lazar A. Phosphoproteome profiling of the macrophage response to different Toll-Like receptor ligands identifies differences in global phosphorylation dynamics. J Proteome Res 2014;13:5185-97.
18. Luber CA, Cox J, Lauterbach H, Fancke B, Selbach M, Tschopp J, et al. Quantitative proteomics reveals subset-specific viral recognition in dendritic cells. Immunity 2010;32:279-89.
19. Meissner F, Scheltema RA, Mollenkopf HJ, Mann M. Direct proteomic quantification of the secretome of activated immune cells. Science 2013;340:475-8.
20. Yu C, Gershwin ME, Chang C. Diagnostic criteria for systemic lupus erythematosus: a critical review. J Autoimmun 2014;48-49:10-3.
21. Lundberg AM, Drexler SK, Monaco O, Williams LM, Sacre SM, Feldmann M, et al. Key differences in TLR3/poly I: C signaling and cytokine induction by human primary cells: a phenomenon absent from murine cell systems. Blood 2007;110:3245-52.
22. Jansen K, Blimkie D, Furlong J, Hajjar A, Rein-Weston A, Crabtree J, et al. Polychromatic flow cytometric high-throughput assay to analyze the innate immune response to Toll-like receptor stimulation. J Immunol Methods 2008;336:183-92.
23. Corbett NP, Blimkie D, Ho KC, Cai B, Sutherland DP, Kallos A, et al. Ontogeny of Toll-like receptor mediated cytokine responses of human blood mononuclear cells. PLoS One 2010;5:e15041.
24. Finck R, Simonds EF, Jager A, Krishnaswamy S, Sachs K, Fantl W, et al. Normalization of mass cytometry data with bead standards. Cytometry 2013;83A:483-94.
25. Bendall SC, Simonds EF, Qiu P, Amir EAD, Krutzik PO, Finck R, et al. Single-cell mass cytometry of differential immune and drug responses across a human hematopoietic continuum. Science 2011;332:687-96.
26. Milush JM, Long BR, Snyder-Cappione JE, Cappione AJ, York VA, Ndhlovu LC, et al. Functionally distinct subsets of human NK cells and monocyte/DC-like cells identified by coexpression of CD56, CD7, and CD4. Blood 2009;114:4823-31.
27. Poli A, Michel T, Thérésine M, Andrès E, Hentges F, Zimmer J. CD56 bright natural killer (NK) cells: an important NK cell subset. Immunology 2009;126:458-65.
28. Dzionek A, Fuchs A, Schmidt P, Cremer S, Zysk M, Miltenyi S, et al. BDCA-2, BDCA-3, and BDCA-4: three markers for distinct subsets of dendritic cells in human peripheral blood. J Immunol 2000;165:6037-46.
29. Liu Y-J. IPC: professional type 1 interferon-producing cells and plasmacytoid dendritic cell precursors. Annu Rev Immunol 2005;23:275-306.
30. Ziegler-Heitbrock L, Ancuta P, Crowe S, Dalod M, Grau V, Hart DN, et al. Nomenclature of monocytes and dendritic cells in blood. Blood 2010;116:e74-80.
31. Hausmann OV, Gentinetta T, Fux M, Ducrest S, Pichler WJ, Dahinden CA. Robust expression of CCR3 as a single basophil selection marker in flow cytometry. Allergy 2010;66:85-91.
32. Finak G, Perez J-M, Weng A, Gottardo R. Optimizing transformations for automated, high throughput analysis of flow cytometry data. BMC Bioinformatics 2010;11:546.
33. Ferwerda G, Meyer-Wentrup F, Kullberg B-J, Netea MG, Adema GJ. Dectin-1 synergizes with TLR2 and TLR4 for cytokine production in human primary monocytes and macrophages. Cell Microbiol 2008;10:2058-66.
34. Bieneman AP, Chichester KL, Chen Y-H, Schroeder JT. Toll-like receptor 2 ligands activate human basophils for both IgE-dependent and IgE-independent secretion. J Allergy Clin Immunol 2005;115:295-301.
35. Sieling PA, Hill PJ, Dobos KM, Brookman K, Kuhlman AM, Fabri M, et al. Conserved mycobacterial lipoglycoproteins activate TLR2 but also require glycosylation for MHC class II-restricted T cell activation. J Immunol 2008;180:5833-42.
36. Chen Q, Davidson TS, Huter EN, Shevach EM. Engagement of TLR2 does not reverse the suppressor function of mouse regulatory T cells, but promotes their survival. J Immunol 2009;183:4458-66.
37. Newell EW, Sigal N, Bendall SC, Nolan GP, Davis MM. Cytometry by time-of-flight shows combinatorial cytokine expression and virus-specific cell niches within a continuum of CD8+ T cell phenotypes. Immunity 2012;36:142-52.
38. Betts MR, Nason MC, West SM, De Rosa SC, Migueles SA, Abraham J, et al. HIV nonprogressors preferentially maintain highly functional HIV-specific CD8+ T cells. Blood 2006;107:4781-9.
39. Koh YT, Scatizzi JC, Gahan JD, Lawson BR, Baccala R, Pollard KM, et al. Role of nucleic acid-sensing TLRs in diverse autoantibody specificities and anti-nuclear antibody-producing B cells. J Immunol 2013;190:4982-90.
40. Guiducci C, Gong M, Cepika AM, Xu Z, Tripodo C, Bennett L, et al. RNA recognition by human TLR8 can lead to autoimmune inflammation. J Exp Med 2013;210:2903-19.
41. Abujam B, Cheekatla S, Aggarwal A. Urinary CXCL-10/IP-10 and MCP-1 as markers to assess activity of lupus nephritis. Lupus 2013;22:614-23.
42. Hasegawa H, Kohno M, Sasaki M, Inoue A, Ito MR, Terada M, et al. Antagonist of monocyte chemoattractant protein 1 ameliorates the initiation and progression of lupus nephritis and renal vasculitis in MRL/lpr mice. Arthritis Rheum 2003;48:2555-66.
43. Marks SD, Williams SJ, Tullus K, Sebire NJ. Glomerular expression of monocyte chemoattractant protein-1 is predictive of poor renal prognosis in paediatric lupus nephritis. Nephrol Dial Transplant 2008;23:3521-6.
44. Kulkarni O, Pawar RD, Purschke W, Eulberg D, Selve N, Buchner K, et al. Spiegelmer inhibition of CCL2/MCP-1 ameliorates lupus nephritis in MRL-(Fas)lpr mice. J Am Soc Nephrol 2007;18:2350-8.
45. Rovin BH. Urine chemokines as biomarkers of human systemic lupus erythematosus activity. J Am Soc Nephrol 2005;16:467-73.
46. Bekeredjian-Ding I, Jego G. Toll-like receptors—sentries in the B-cell response. Immunology 2009;128:311-23.
47. Martinez J, Huang X, Yang Y. Direct TLR2 signaling is critical for NK cell activation and function in response to vaccinia viral infection. PLoS Pathog 2010;6:e1000811.
48. Esin S, Counoupas C, Aulicino A, Brancatisano FL, Maisetta G, Bottai D, et al. Interaction of *Mycobacterium tuberculosis* cell wall components with the human natural killer cell receptors NKp44 and Toll-like receptor 2. Scand J Immunol 2013;77:460-9.
49. Marcenaro E, Ferranti B, Falco M, Moretta L, Moretta A. Human NK cells directly recognize *Mycobacterium bovis* via TLR2 and acquire the ability to kill monocyte-derived DC. Int Immunol 2008;20:1155-67.
50. Lancioni CL, Li Q, Thomas JJ, Ding X, Thiel B, Drage MG, et al. *Mycobacterium tuberculosis* lipoproteins directly regulate human memory CD4+ T cell activation via Toll-like receptors 1 and 2. Infect Immun 2011;79:663-73.
51. Shireman PK, Contreras-Shannon V, Ochoa O, Karia BP, Michalek JE, McManus LM. MCP-1 deficiency causes altered inflammation with impaired skeletal muscle regeneration. J Leukoc Biol 2006;81:775-85.
52. Kim RY, Hoffman AS, Itoh N, Ao Y, Spence R, Sofroniew MV, et al. Astrocyte CCL2 sustains immune cell infiltration in chronic experimental autoimmune encephalomyelitis. J Neuroimmunol 2014;274:53-61.
53. Atamas SP, White B. The role of chemokines in the pathogenesis of scleroderma. Curr Opin Rheumatol 2003;15:772-7.
54. Brenner M, Laragione T, Gulko PS. Analyses of synovial tissues from arthritic and protected congenic rat strains reveal a new core set of genes associated with disease severity. Physiol Genomics 2013;45:1109-22.
55. Bauer JW, Baechler EC, Petri M, Batliwalla FM, Crawford D, Ortmann WA, et al. Elevated serum levels of interferon-regulated chemokines are biomarkers for active human systemic lupus erythematosus. PLoS Med 2006;3:e491.
56. Pascual V, Allantaz F, Patel P, Palucka AK, Chaussabel D, Banchereau J. How the study of children with rheumatic diseases identified interferon-α and interleukin-1 as novel therapeutic targets. Immunol Rev 2008;223:39-59.
57. O'Gorman WE, Huang H, Wei Y-L, Davis KL, Leipold MD, Bendall SC, et al. The split virus influenza vaccine rapidly activates immune cells through Fcγ receptors. Vaccine 2014;32:5989-97.